Distinct roles of stereociliary links in the nonlinear sound processing and noise resistance of cochlear outer hair cells

Woongsu Han[a,b,1], Jeong-Oh Shin[c,1], Ji-Hyun Ma[c,1], Hyehyun Min[c,d], Jinsei Jung[b,e], Jinu Lee[f], Un-Kyung Kim[g], Jae Young Choi[b,e], Seok Jun Moon[h], Dae Won Moon[i,2], Jinwoong Bok[b,c,d,e,2], and Chul Hoon Kim[a,b,d,2]

[a]Department of Pharmacology, Yonsei University College of Medicine, 03722 Seoul, Korea; [b]Brain Korea 21 Project for Medical Science, Yonsei University College of Medicine, 03722 Seoul, Korea [c]Department of Anatomy, Yonsei University College of Medicine, 03722 Seoul, Korea; [d]Severance Biomedical Science Institute, Yonsei University College of Medicine, 03722 Seoul, Korea; [e]Department of Otorhinolaryngology, Yonsei University College of Medicine, 03722 Seoul, Korea; [f]Yonsei Institute of Pharmaceutical Sciences, College of Pharmacy, Yonsei University, 21983 Inchon, Korea; [g]Department of Biology, Kyungpook National University, 41566 Daegu, Korea; [h]Department of Oral Biology, Yonsei University College of Dentistry, 03722 Seoul, Korea; and [i]Department of New Biology, Daegu Gyeongbuk Institute of Science and Technology, 42988 Daegu, Korea

Edited by David P. Corey, Harvard Medical School, Boston, MA, and accepted by Editorial Board Member J. Anthony Movshon March 20, 2020 (received for review November 17, 2019)

Outer hair cells (OHCs) play an essential role in hearing by acting as a nonlinear amplifier which helps the cochlea detect sounds with high sensitivity and accuracy. This nonlinear sound processing generates distortion products, which can be measured as distortion-product otoacoustic emissions (DPOAEs). The OHC stereocilia that respond to sound vibrations are connected by three kinds of extracellular links: tip links that connect the taller stereocilia to shorter ones and convey force to the mechanoelectrical transduction channels, tectorial membrane-attachment crowns (TM-ACs) that connect the tallest stereocilia to one another and to the overlying TM, and horizontal top connectors (HTCs) that link adjacent stereocilia. While the tip links have been extensively studied, the roles that the other two types of links play in hearing are much less clear, largely because of a lack of suitable animal models. Here, while analyzing genetic combinations of *tubby* mice, we encountered models missing both HTCs and TM-ACs or HTCs alone. We found that the *tubby* mutation causes loss of both HTCs and TM-ACs due to a mislocalization of stereocilin, which results in OHC dysfunction leading to severe hearing loss. Intriguingly, the addition of the modifier allele *modifier of tubby hearing 1* in *tubby* mice selectively rescues the TM-ACs but not the HTCs. Hearing is significantly rescued in these mice with robust DPOAE production, indicating an essential role of the TM-ACs but not the HTCs in normal OHC function. In contrast, the HTCs are required for the resistance of hearing to damage caused by noise stress.

hearing loss | outer hair cell | stereocilia | tubby | stereocilin

Outer hair cells (OHCs) in the cochlea act as a cochlear amplifier, making the cochlea a highly sensitive and accurate sound processor. Abnormal OHC function leads to severe hearing loss due to decreased sensitivity and impaired sound-evoked neural activity (1). OHCs possess actin filament-rich protrusions called stereocilia on their apical surface. These stereocilia are arranged in a three-row staircase pattern with the taller ones connected to adjacent shorter stereocilia by filamentous specializations called tip links (2). Sound vibrations deflect the stereocilia, pulling on the tip links to open mechanoelectrical transduction (MET) channels situated in the shorter stereocilia (2). Stereocilia deflection initiates an amplification process in the OHCs that depends on positive feedback driven by membrane-based somatic electromotility and active stereociliary bundle motility (2, 3). The amplified sound signal is then transmitted to the brain via neural activity elicited by the inner hair cells (IHCs). This amplification process in the OHCs is nonlinear, meaning that the degree of amplification varies depending on the intensity and frequency of the incoming sound (2, 3). This nonlinear signal processing can create cross-frequency interactions, which help sharpen frequency selectivity and are critical for the perception of complex sounds such as speech (4). Cross-frequency interactions also generate cochlear distortions, which can be noninvasively measured as distortion product otoacoustic emissions (DPOAEs). These are considered a reflection of normal OHC function (5).

In addition to the tip links, mature OHC stereocilia have two additional cell-surface specializations (6). The horizontal top connectors (HTCs) are zipper-like structures present just below the tip links that connect adjacent stereocilia within and across rows. Tectorial membrane-attachment crowns (TM-ACs) are present at the tips of the tallest stereocilia to couple them to one another laterally and to the overlying gelatinous TM. Thus, mature OHC stereocilia are interconnected and supported mainly by three types of extracellular link structures: the tip links, the HTCs, and the TM-ACs. All three of these types of links are considered essential for normal OHC function and DPOAE production (7).

Although the molecular constituents and mechanisms governing the tip links have been extensively investigated (2), the

Significance

Our hearing organ, the cochlea, acts as an active sound amplifier rather than a simple detector due to the action of outer hair cells (OHCs). This active sound processing by OHCs requires specific hair bundle architecture in which stereocilia are connected to each other and to the overlying tectorial membrane by nanoscale extracellular links. But it remains unclear how these stereociliary links contribute to OHC function. Using *tubby* mouse genetics, we dissected the role of each link in OHC function. While the links connecting stereocilia and the tectorial membrane are essential for normal OHC function, the links connecting adjacent stereocilia together are more important for preventing hearing loss due to noise stress.

Author contributions: D.W.M., J.B., and C.H.K. designed research; W.H., J.-O.S., J.-H.M., and H.M. performed research; J.L. and D.W.M. contributed new reagents/analytic tools; W.H., J.-O.S., J.-H.M., H.M., J.J., U.-K.K., J.Y.C., S.J.M., J.B., and C.H.K. analyzed data; and D.W.M., J.B., and C.H.K. wrote the paper.

The authors declare no competing interest.

This article is a PNAS Direct Submission. D.P.C. is a guest editor invited by the Editorial Board.

[1]W.H., J.-O.S., and J.-H.M. contributed equally to this work.

[2]To whom correspondence may be addressed. Email: dwmoon@dgist.ac.kr, bokj@yuhs.ac, or kimhoon@yuhs.ac.

This article contains supporting information online at https://www.pnas.org/lookup/suppl/doi:10.1073/pnas.1920229117/-/DCSupplemental.

First published May 1, 2020.

roles of the TM-ACs and HTCs in OHC function remain unclear. This is mainly due to a scarcity of knowledge about their molecular constituents and a lack of suitable animal models without these specific links. Thus far, only a few mouse models have reportedly been used for the study of the molecular architecture and function of these two links (8–11). *Tecta* functional null mutant mice provide an animal model in which the tips of OHC stereocilia are exposed to the endolymphatic fluid instead of being embedded in the TM (8, 9). In *Tecta* mutant mice, DPOAEs are generated in response to high-intensity sounds but not to low-intensity sounds, suggesting that the function of the cochlear amplifier is affected, yet the components involved in nonlinear sound processing in the OHCs are preserved (9). In *stereocilin* knockout (*Strc* KO) mice, which lack both TM-ACs and HTCs, the OHC stereocilia are connected neither to one another nor to the TM (10, 11). These mice do not generate DPOAEs, even in response to high-intensity sounds, suggesting a fundamental disruption of the components involved in the OHC's nonlinear sound processing (11). Based on these results, the HTCs were proposed to be an essential component of the nonlinear sound processing that creates DPOAEs (11). However, it has been difficult to directly investigate the specific roles that the HTCs play in hearing because there were no animal models lacking only the HTCs.

A spontaneous mutation in the *tubby* gene was discovered 40 y ago that causes obesity, retinal degeneration, and hearing loss in mice (12, 13). The *tubby* mouse has a loss-of-function mutation in the *tubby* gene—a spontaneous G-to-T transversion at a splicing donor site that leads to the replacement of 44 carboxyl-terminal amino acids of the tubby (TUB) protein with 24 intron-encoded amino acids (14, 15). TUB protein's conserved C-terminal tubby region contains a putative DNA-binding domain and a phosphatidylinositol 4,5-bisphosphate (PIP_2)-binding region that determines its intracellular localization to the surface membrane (16). TUB's N-terminal domain contains a nuclear localization signal and an intraflagellar transport-A (IFT-A)-binding domain (17, 18). Some have proposed that TUB acts as a transcription factor (19), but others have suggested roles in G-protein–coupled receptor (GPCR) signaling (16), postsynaptic signaling (20), phagocytosis (21), insulin signaling (22), endocytosis (23), and ciliary transport (24, 25). None of these, however, sufficiently explain the pathogenesis of the *tubby* phenotypes.

Hearing loss in *tubby* mice appears at 3 wk of age and then grows progressively worse (13). Degeneration of IHCs, OHCs, and spiral ganglion neurons (SGNs) occurs starting from the basal end of the cochlea at 1 mo of age and then gradually progresses toward the apex. OHC loss progresses to the middle turn by 6 mo of age, whereas IHC and SGN losses are limited to the basal turn (13, 26, 27). Since hearing loss is already apparent in all frequency ranges as early as 3 wk of age when there is no evident loss of HCs and SGNs, the degenerative process is unlikely to be the primary cause of hearing loss in *tubby* mice.

While investigating the pathogenesis of the hearing loss of *tubby* mice, we found that *tubby* mice lose two extracellular links from their OHC stereocilia—the HTCs and the TM-ACs—mimicking the phenotypes of *Strc* KO mice. Unexpectedly, we were able to selectively rescue the TM-ACs but not the HTCs in *tubby* mice by adding a modifier allele known as "*modifier of tubby hearing 1*" (*moth1*) (20, 28). These models provided us with a unique opportunity to study the function of each of these stereociliary links in hearing. Our results indicate that the TM-ACs but not the HTCs are essential for normal OHC function as a nonlinear sound processor and that the HTCs play a critical role in protecting stereocilia from intense noise exposure.

Results

Hearing Loss in *Tubby* Mice Is Due to OHC Defects. Consistent with a previous report (13), we found that auditory brainstem response (ABR) thresholds are increased by 40 to 50 dB SPL at all frequencies in 3-wk-old homozygous *tubby* mice (Fig. 1*A*). This result indicates a significant reduction in hearing sensitivity, which is often the result of a failure of OHC function. We tested this idea by measuring DPOAEs in *tubby* mice. DPOAEs reflect nonlinear sound processing by OHCs, which is necessary for the cochlea to detect sounds with high sensitivity and accuracy (7). DPOAEs are completely abolished in *tubby* mice (Fig. 1*B*), suggesting that OHC dysfunction is the major cause of their hearing loss. Consistent with this hypothesis, scanning electron microscopy (SEM) showed that rows of stereocilia in the OHCs of *tubby* mice are not as tightly associated with one another as those of wild-type mice at postnatal day 21 (P21) (Fig. 1 *C–F*). This stereociliary disarrangement is already apparent at P16 (*SI Appendix*, Fig. S1 *C–F*). In higher magnification SEM images and helium ion microscope (HIM) images, we found a loss of the HTCs that link adjacent stereocilia (Fig. 1 *I* and *J* and *SI Appendix*, Fig. S1 *E–J*). In contrast, the tip links that are essential for the opening of MET channels in response to sound stimuli are preserved in *tubby* mice (Fig. 1 *J* and *N*). We confirmed the absence of HTCs and the presence of tip links in *tubby* mice by transmission electron microscopy (Fig. 1 *K* and *L*). In addition, we found that *tubby* mice lack the TM-ACs that connect the tallest stereocilia to the TM (Fig. 1 *M* and *N*). Correspondingly, the imprints on the undersurface of the TM, which reflect points of physical contact between the tallest stereocilia and the TM, are also absent in *tubby* mice (Fig. 1 *O* and *P*). We were unable, however, to observe any defects in the stereociliary structure of the IHCs (Fig. 1 *G* and *H*) or any disruption of the overall architecture of the organ of Corti in most cochlear regions of *tubby* mice until at least P21 (Fig. 1 *C* and *D* and *SI Appendix*, Fig. S2). These results indicate that TUB plays an essential role in the stereociliary structure and function of OHCs.

TUB Is Localized at the Tips of OHC Stereocilia. This discovery of the site of the hearing defect in *tubby* mice (Fig. 1) prompted us to examine TUB protein localization in the organ of Corti. To this end, we generated a TUB-specific polyclonal antibody to visualize the cellular and subcellular localization of TUB proteins. Other groups have reported diffuse TUB immunoreactivity in the IHCs, OHCs, Deiter's cells, outer phalangeal cells, and SGNs (28). We found, however, that TUB immunoreactivity is limited to the tips of OHC stereocilia in wild-type mice at P21 (Fig. 2 *A* and *E*) and is completely absent from *tubby* mutant mice (Fig. 2*B* and *SI Appendix*, Fig. S3 *A* and *B*). We were unable to detect TUB protein in the IHCs (Fig. 2 *A* and *F*) or the vestibular hair cells (Fig. 2 *G* and *H*). TUB immunoreactivity is first detectable at P5 in the tallest row of stereocilia, but it spreads to the intermediate and shortest rows by P21 (Fig. 2 *C–E*). Next we examined whether TUB localization to the tips of OHC stereocilia is dependent on PIP_2 (16, 18). Treating wild-type whole cochlear explants with phenylarsine oxide, an inhibitor of PIP_2 synthesis, results in the disappearance of TUB proteins from the stereocilia tips of OHCs (*SI Appendix*, Fig. S4). This suggests that the regulation of TUB localization to the tips of the stereocilia is complex and PIP_2 dependent.

The Maintenance of Stereocilin Localization Depends on TUB Function. Stereocilin (STRC) is a stereociliary protein mutated in human hereditary deafness DFNB16, and mice lacking *stereocilin* also show deafness (11, 29). STRC is localized to the tips of OHC stereocilia and is an essential component of the HTCs and TM-ACs (10, 11). Interestingly, the phenotypes of *Strc* knockout mice closely resemble those of *tubby* mice in several aspects: both mutant mice show 1) loss of the HTCs and TM-ACs, 2) preservation of the tip links, and 3) loss of DPOAE production (Fig. 1) (10, 11). Consistent with these results, we found both TUB and STRC proteins are located at the tips of OHC

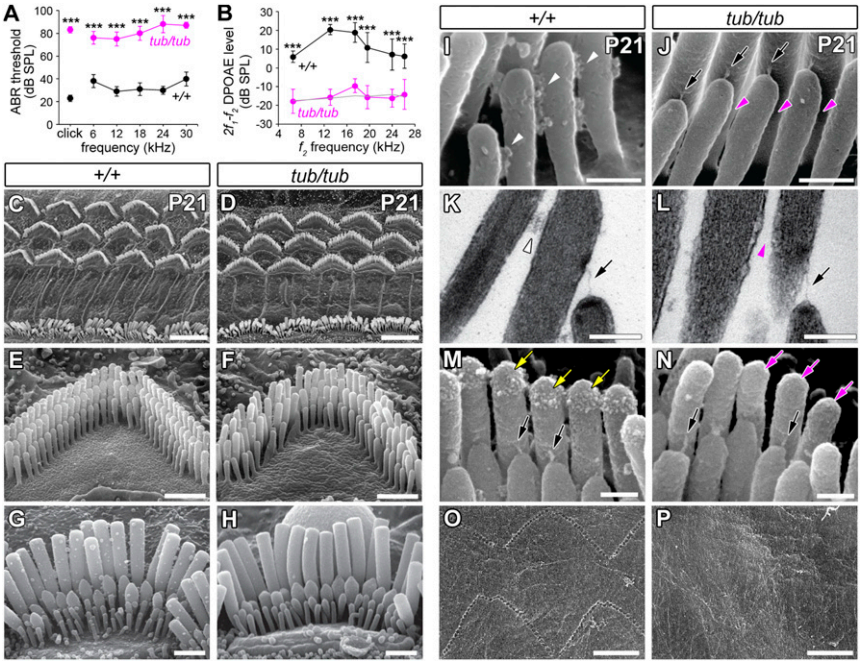

Fig. 1. Hearing loss in *tubby* mice results from OHC defects. (*A* and *B*) ABR thresholds and DPOAE amplitudes in $^{+/+}$ and *tub/tub* mice at 3 wk of age ($n = 5$). Values and error bars reflect mean ± SD. Statistical comparisons were made with two-way ANOVA with Bonferroni corrections for multiple comparisons (***$P < 0.001$) at each frequency between $^{+/+}$ and *tub/tub* mice. (*C–H*) SEM images of the inner and outer hair cells in $^{+/+}$ and *tub/tub* mice at P21. (*I–N*) HIM (*I* and *J*), TEM (*K* and *L*), and SEM (*M* and *N*) images of OHC stereocilia in $^{+/+}$ and *tub/tub* mice at P21. White arrowheads indicate HTCs, and magenta arrowheads indicate sites at which HTCs would normally be located. Tip links are indicated by black arrows. Yellow and magenta arrows indicate the tips of the tallest stereocilia with or without the TM-ACs, respectively. (*O* and *P*) SEM images of the imprints on the undersurface of the TM in $^{+/+}$ and *tub/tub* mice at P21. (Scale bars: 5 μm, *C* and *D*; 1 μm, *E*, *F*, *O*, and *P*; 0.2 μm, *G–N*.)

stereocilia in wild-type mice at P21 (Fig. 2 *A*, *E*, *I*, and *M*). Similar to TUB, STRC is initially localized to the tips of the tallest OHC stereocilia in P5 wild-type mice (Fig. 2*K*), subsequently spreading to the intermediate and shorter stereocilia by P21 (Fig. 2 *K–M*). We also observed nearly identical time courses for the onset and expression patterns of TUB and STRC proteins when we examined them, respectively, in the right and left cochlea isolated from the same mice (*SI Appendix*, Fig. S5). In *tubby* mice, surprisingly, although STRC is initially localized to the tallest stereocilia at P5 (Fig. 2*N*), it disappears from OHC stereocilia by P9 and remains undetectable at P21 (Fig. 2 *J*, *O*, and *P*). In contrast, the localization of STRC in the kinocilia of the OHCs (Fig. 2*N*) and vestibular hair cells (*SI Appendix*, Fig. S6) is unaffected by the *tubby* mutation. This indicates that the maintenance of STRC at the tips of OHC stereocilia is dependent on TUB function and that the requirement for TUB in STRC localization is specific to OHC stereocilia. Using in situ hybridization, we observed that *Strc* messenger RNAs (mRNAs) are specifically expressed in hair cells in both wild-type and *tubby* mice (Fig. 2 *Q–U*). In addition, we found no difference between wild-type and *tubby* mice when we performed a real-time PCR analysis of *Strc* mRNA levels in the cochlea, suggesting that *Strc* transcription is not regulated by TUB (Fig. 2*V*). The localization of prestin, which is essential for the electromotility of the OHCs (30), also appears normal in *tubby* mice (*SI Appendix*, Fig. S7). Together, these data indicate that the hearing loss of *tubby* mice is caused by a failure in the maintenance of STRC at the tips of OHC stereocilia, leading to their structural and functional defects.

Rescue of *tubby* Hearing by *moth1* Is Accompanied by a Restoration of OHC Function. The hearing loss of mice carrying the *tubby* mutation, which originally arose in the C57BL/6J genetic background, is rescued by crossing such mice with the AKR/J, CAST/Ei, or 129/Ola strains (28) (Fig. 3*A*). These strains have a sequence polymorphism in the *Map1a* gene that is referred to as *moth1* (20). The presence of *moth1* restores the hearing loss of *tubby* mice by an unknown mechanism. We took advantage of this unique phenomenon to address the question of whether and how STRC mediates TUB function in the OHCs. We crossed *tubby* mice in the C57BL/6J background (*tub*/*tub*; $Map1a^{B6}$) with AKR/N mice to generate mice carrying both the *tubby* mutation and the protective *Map1a* allele (*tub*/*tub*; $Map1a^{AKR}$). Consistent with previous reports (20, 28), the ABR thresholds of *tub*/*tub*; $Map1a^{AKR}$ mice were significantly improved compared with those of *tub*/*tub*; $Map1a^{B6}$ mice at all frequencies examined except for 30 kHz at P21 (Fig. 3*B*). We found that the DPOAE amplitudes of *tub*/*tub*; $Map1a^{AKR}$ mice are also significantly increased compared with those of *tub*/*tub*; $Map1a^{B6}$ mice, except at higher frequencies (Fig. 3 *C* and *D*). Since the rescue of hearing appeared incomplete at higher frequencies, unlike what had been previously reported (28), we extended our analysis to *tub*/*tub*; $Map1a^{AKR}$ mice at P15, the time of hearing onset, and found that ABR thresholds and DPOAE amplitudes are similar to those of wild-type mice at all frequencies examined (*SI Appendix*, Fig. S8 *A* and *B*). The input/output functions of DPOAE amplitudes at a low-frequency (12 kHz) f_2 and a high-frequency (24 kHz) f_2 also show no significant difference between *tub*/*tub*; $Map1a^{AKR}$ and wild-type mice for all stimulus levels (*SI Appendix*, Fig. S8 *C* and *D*). This suggests that hearing is rescued by the modifier $Map1a^{AKR}$ allele even at higher frequencies at early ages. The later increase in ABR threshold at frequencies above 12 kHz by P21 implies that HTCs may also contribute to long-term maintenance of hair bundle structure. Collectively, these ABR and DPOAE results suggest the rescue of hearing in *tub*/*tub*; $Map1a^{AKR}$ mice is accompanied by a restoration of OHC function.

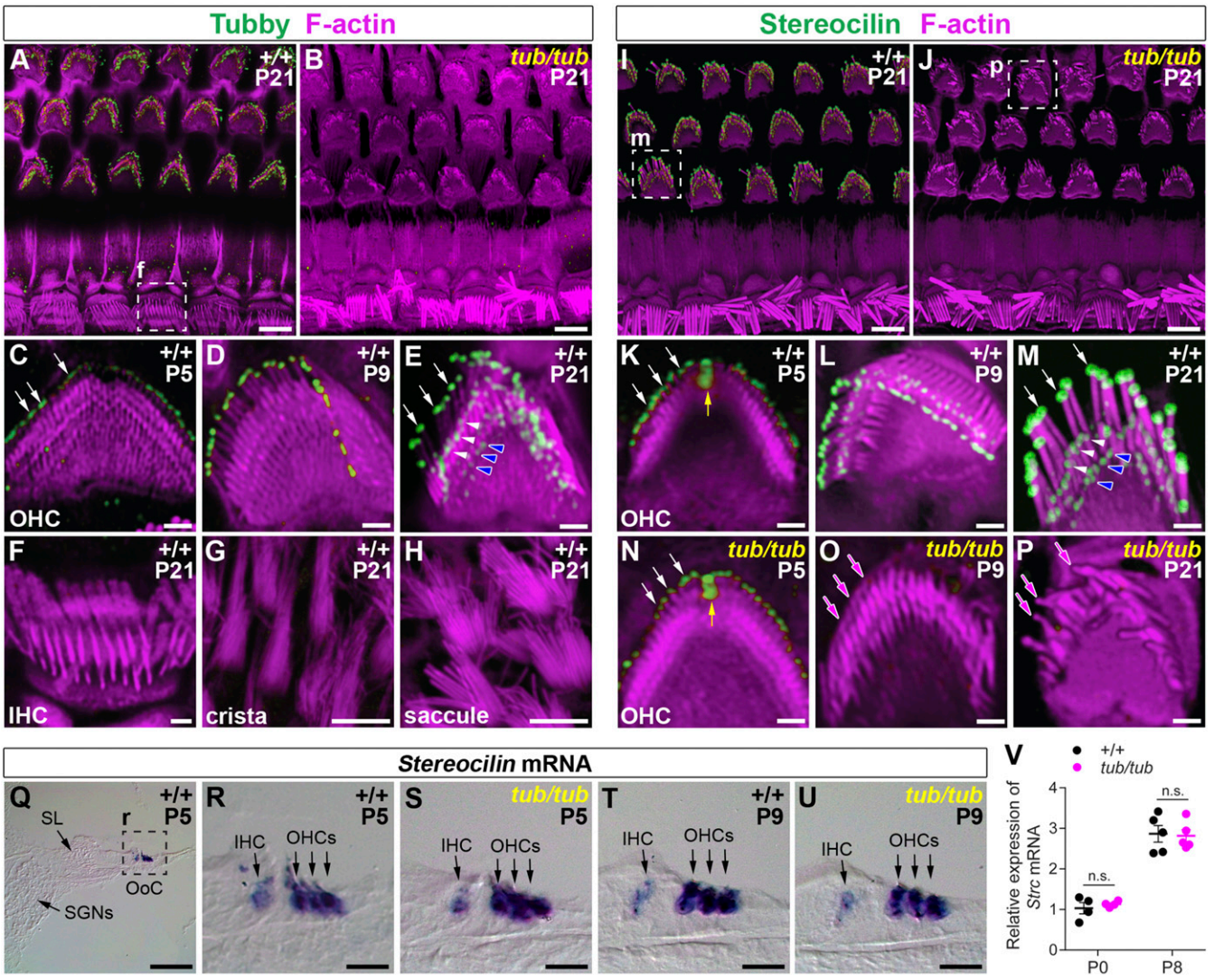

Fig. 2. TUB is required for the maintenance of STRC localization to the tips of OHC stereocilia. (*A* and *B*) Immunofluorescence images of the organ of Corti labeled with a TUB antibody (green) and phalloidin (magenta) in $^{+/+}$ (*A*) and *tub/tub* (*B*) mice at P21. (*C–E*) Developmental series of TUB localization in the OHC stereocilia at P5 (*C*), P9 (*D*), and P21 (*E*). (*F–H*) The absence of tubby immunoreactivity in IHCs (*F*) and hair cells of the crista (*G*) and saccule (*H*). The IHC image in *F* was magnified from the image in *A* and rotated 180° to appear in its correct orientation. (*I* and *J*) Immunofluorescence images of the organ of Corti labeled with a STRC antibody (green) and phalloidin (magenta) in $^{+/+}$ (*I*) and *tub/tub* (*J*) mice at P21. (*K–P*) Developmental series of STRC localization in OHC stereocilia in $^{+/+}$ (*K–M*) and *tub/tub* (*N–P*) mice at P5 (*K* and *N*), P9 (*L* and *O*), and P21 (*M* and *P*). White arrows indicate the tallest stereocilia, and white and blue arrowheads indicate the second and third rows of stereocilia, respectively. Yellow arrows indicate kinocilia (*K* and *N*). The absence of STRC in the tallest stereocilia is indicated by magenta arrows (*O* and *P*). (*Q–U*) Images of in situ hybridizations showing the regions of *Strc* mRNA expression in the organ of Corti of $^{+/+}$ (*Q*, *R*, and *T*) and *tub/tub* (*S* and *U*) mice at P5 (*Q–S*) and P9 (*T* and *U*). (*V*) Quantitative real-time PCR analyses showing relative expression levels of *Strc* mRNAs in $^{+/+}$ and *tub/tub* mice at P0 ($n = 4$) and P8 ($n = 5$). Statistical significance was determined using two-tailed Student's *t* test (n.s.: nonsignificant, $P > 0.05$). OHC, outer hair cell; IHC, inner hair cell; SL, spiral limbus; SGNs, spiral ganglion neurons; OoC, organ of Corti. (Scale bars: 5 μm, *A*, *B*, and *G–J*; 1 μm, *C–F* and *K–P*; 100 μm, *Q*; and 20 μm, *R–U*.)

Horizontal Top Connectors Are Nonessential for Nonlinear Cochlear Signal Processing. We therefore compared the structure of the OHC stereocilia of *tub/tub*; *Map1a*^{B6} mice and *tub/tub*; *Map1a*^{AKR} mice. In *tub/tub*; *Map1a*^{B6} mice, the HTCs and the TM-ACs in OHC stereocilia and the imprints on the undersurface of the TM are lost (Fig. 3 *E–G* and *K–M* and *SI Appendix*, Fig. S9 *A–F*). Presumably, this occurs because formation of both the TM-ACs and HTCs is dependent on STRC (10, 11). Interestingly, in *tub/tub; Map1a*^{AKR} mice, the TM-ACs at the stereocilia tips and the imprints on the TM are rescued, but the HTCs are still missing (Fig. 3 *Q–S* and *SI Appendix*, Fig. S9 *G–I*). In an immunofluorescence analysis, we found that STRC localization is rescued only to the tallest row of stereocilia, not the intermediate or shortest rows (Fig. 3 *H*, *N*, and *T* and *SI Appendix*, Fig. S10). Using an immunogold analysis, we confirmed the finding that STRC localization is rescued in *tub/tub; Map1a*^{AKR} mice to the tallest stereocilia tips (Fig. 3 *I*, *O*, and *U* and *SI Appendix*, Fig. S9 *P–R*) and to the TM imprints (Fig. 3 *J*, *P*, and *V*). These results suggest that the rescue of hearing in *tub/tub; Map1a*^{AKR} mice is due to the selective rescue of STRC to the tallest stereocilia, which then permits coupling between the tallest stereocilia and the TM; the rescue might be further strengthened by STRC's possible role in interconnecting the stereocilia laterally and thereby organizing the tallest rows in a regular pattern.

This rescue of hearing in the absence of the HTCs (Fig. 3) is surprising because the HTCs were considered essential in normal hearing. They were proposed to govern the coherent motion of the OHC stereocilia bundles that ensures the concerted gating of

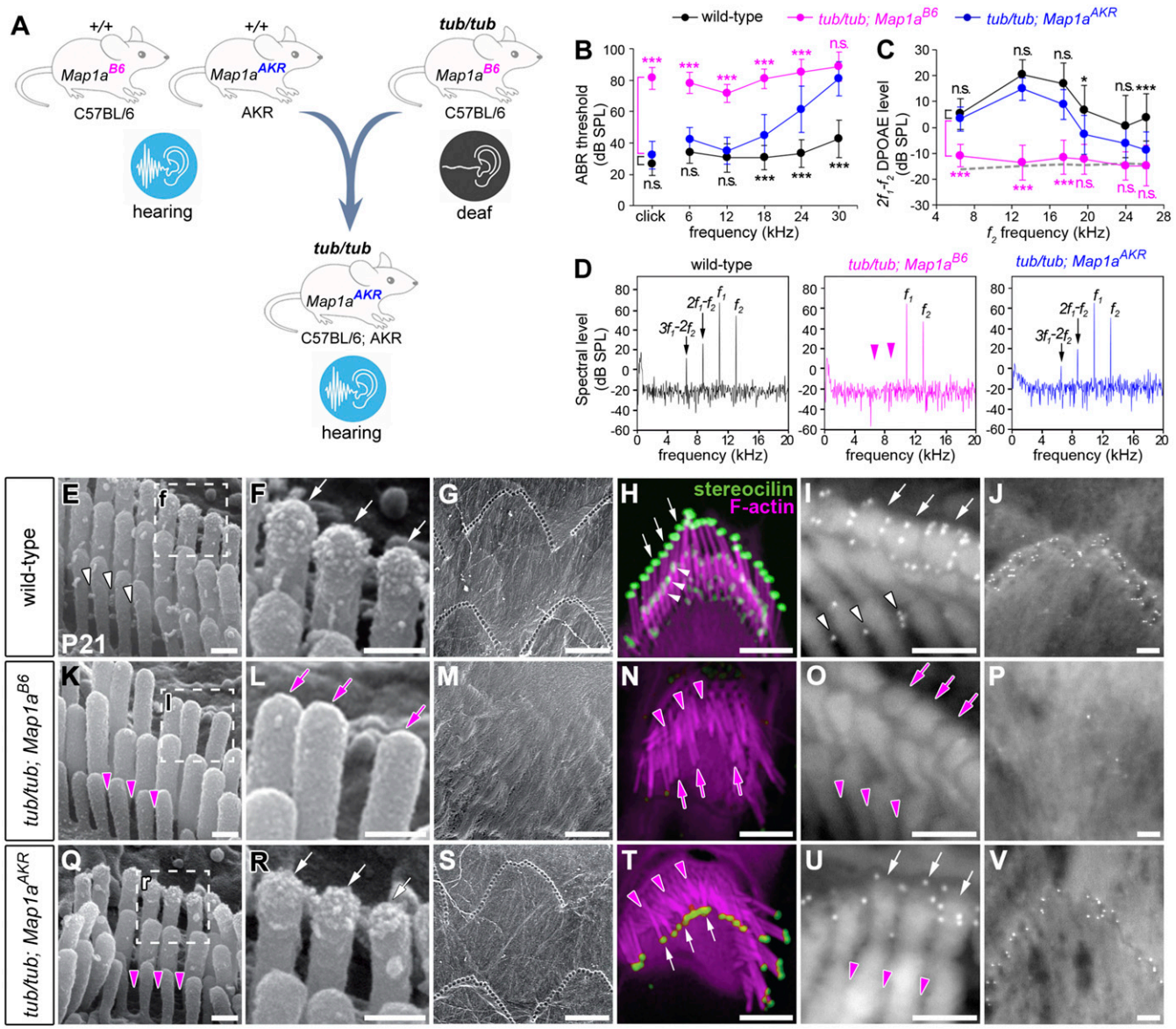

Fig. 3. Hearing is rescued in *tub/tub; Map1a*^{AKR} mice by the selective preservation of the TM-ACs. (*A*) A diagram illustrating the rescue of hearing for *tub/tub* mice of the C57BL/6 strain by crossing them with mice of the AKR strain carrying the modifier *Map1a* allele (*Map1a*^{AKR}). Both $^{+/+}$*; Map1a*^{B6} and $^{+/+}$*; Map1a*^{AKR} mice show normal hearing, and both genotypes are used as wild type. (*B* and *C*) ABR thresholds (*B*) and DPOAE amplitudes (*C*) of wild-type ($n = 31$), *tub/tub; Map1a*^{B6} ($n = 12$), and *tub/tub; Map1a*^{AKR} ($n = 18$) mice at 3 wk. Values and error bars reflect means ± SD. Statistical comparisons were made with two-way ANOVA using Bonferroni corrections for multiple comparisons (*$P < 0.05$, ***$P < 0.001$; n.s.: nonsignificant [$P > 0.05$]). Black and magenta symbols indicate statistical significance at each frequency between wild-type and *tub/tub; Map1a*^{AKR} mice and between *tub/tub; Map1a*^{B6} and *tub/tub; Map1a*^{AKR} mice, respectively. (*D*) Representative frequency spectrum of the ear-canal signal showing the primary tones f_1 and f_2 and DPOAEs at $2f_1$-f_2 and $3f_1$-$2f_2$ frequencies. (*E*, *F*, *K*, *L*, *Q*, and *R*) SEM images of OHC stereocilia in the midcochlear region of wild-type, *tub/tub; Map1a*^{B6}, and *tub/tub; Map1a*^{AKR} mice at 3 wk. The presence and absence of TM-ACs in the tallest stereocilia rows are indicated by white and magenta arrows, respectively. White arrowheads indicate HTCs and magenta arrowheads indicate sites at which HTCs would normally be located. (*G*, *M*, and *S*) SEM images showing the imprints on the undersurface of the TM in wild-type (*G*), *tub/tub; Map1a*^{B6} (*M*), and *tub/tub; Map1a*^{AKR} (*S*) mice. (*H*, *N*, and *T*) Immunofluorescence images of OHC stereocilia labeled with a STRC antibody (green) and phalloidin (magenta) at P21. The presence and absence of STRC at the tallest stereocilia are indicated by white and magenta arrows, respectively. The presence and absence of STRC in the lower stereocilia rows are indicated by white and magenta arrowheads, respectively. (*I*, *J*, *O*, *P*, *U*, and *V*) Immunogold SEM images visualizing STRC localization in OHC stereocilia (*I*, *O*, and *U*) and TM imprints (*J*, *P*, and *V*) in the midcochlear region. (Scale bars: 0.2 μm, *E*, *F*, *I*–*L*, *O*–*R*, *U*, and *V*; and 1 μm, *G*, *H*, *M*, *N*, *S*, and *T*.)

MET channels (31, 32) and to provide the structural basis for the production of DPOAE (11). Our results suggest instead that the HTCs are dispensable for the nonlinear signal processing by OHCs and the subsequent production of DPOAE.

Horizontal Top Connectors Are Required for Noise-Resistant Hearing. What role, then, do the HTCs play in auditory function? They are thought to maintain the mechanical stability of stereocilia bundles against noise trauma (33, 34). This hypothesis, however, remains untested due to a lack of suitable animal models missing only the HTCs. We, therefore, examined this possibility using noise-exposed wild-type, *tub/tub*; *Map1a*^{B6}, and *tub/tub*; *Map1a*^{AKR} mice. As expected, noise exposure (broadband noise in the 2- to 20-kHz frequency range at 105 dB SPL for 2 h) dramatically increases ABR thresholds in response to click (Fig. 4*A*) and pure tone (*SI Appendix*, Fig. S11 *A*–*C*) stimuli in all three genotypes.

However, while we observed a significant improvement in the ABR thresholds of wild-type mice over the course of 14 d, we saw no such improvement in *tub*/*tub*; *Map1a*^{B6} and *tub*/*tub*; *Map1a*^{AKR} mice (Fig. 4*A* and *SI Appendix*, Fig. S11 *A*–*C*). Similarly, noise-induced reductions in DPOAE amplitudes in response to pure tone (Fig. 4*B* and *SI Appendix*, Fig. S11 *D*–*F*) stimuli were significantly reversed 14 d later in wild type, but not in *tub*/*tub*; *Map1a*^{B6} or in *tub*/*tub*; *Map1a*^{AKR} mice. Correspondingly, the TM-ACs and the TM imprints were preserved after noise exposure in wild-type mice, but they disappeared or became less distinct in *tub*/*tub; Map1a*^{AKR} mice (Fig. 4 *C*–*N*; images from midcochlea). These results suggest that, as was previously proposed (33, 34), the mechanical stability of stereocilia bundles weakens in the absence of structural support provided by the HTCs that connect the stereocilia together as a unit and prevent the stereocilia from splaying. This role for the HTCs may prevent the stereocilia from splaying against mechanical stress and from easy detachment from the TM. We cannot exclude the possibility, however, that the rescued TM-ACs are more or less different in quality from those of wild types, making the coupling between stereocilia and the TM less stable.

Discussion

Our study indicates that TUB protein plays an important role in OHC function by maintaining STRC localization at the tips of stereocilia as well as the integrity of the STRC-dependent stereociliary links—the HTCs and TM-ACs (Fig. 5). The *tub*/*tub*; *Map1a*^{AKR} mice provided us with an unprecedented opportunity to determine the roles that these stereociliary links play in hearing. We found that the TM-ACs that couple the tallest stereocilia to the TM are essential in hearing sensitivity and for generating the distortion products (DPOAEs) that reflect normal OHC function. In contrast, the HTCs are required for noise-resistant hearing (Fig. 5).

Our results appear to conflict with those of Verpy et al., who studied *Strc* KO mice and proposed that the HTCs are required for cochlear distortion (11). Their conclusion included the assumption that the TM-ACs that connect OHC stereocilia to the TM are dispensable for cochlear distortion. This assumption grew out of the prior observation that *Tecta* functional null mutant mice, the stereocilia of which are detached from the TM, still produce DPOAEs, albeit only in response to high-intensity sounds (9). However, *Strc* KO mice lose both the HTCs and the TM-ACs, completely abolishing DPOAE production. Thus, it remained unclear whether the HTCs are essential for cochlear distortion because there was not yet any animal model lacking only the HTCs. Here, in this study, we directly address this issue with *tub*/*tub*; *Map1a*^{AKR} mice, which lose their HTCs, but not their TM-ACs. The robust production of DPOAEs in *tub*/*tub*; *Map1a*^{AKR} mice makes it clear that HTCs are dispensable for cochlear distortion. In addition, these mice show a rescue of hearing sensitivity—as evidenced by their reduced ABR thresholds—accompanied by a selective preservation of STRC in the TM-ACs. These results suggest the TM-ACs are more important for generating cochlear distortion and cochlear amplification than the HTCs. We cannot exclude the possibility, however, that the HTCs are involved in the generation of DPOAEs when both the HTCs and the TM-ACs are intact. Still, if HTCs have one at all, we expect their contribution to be small. Although we were unable in this study to quantify the extent to which the TM-ACs contribute to the generation of DPOAEs directly, we are still interested in clarifying the origin of cochlear distortion. Our study does provide a useful starting point for future research because we were able to confirm the finding that cochlear distortion requires STRC (11). Further studies of STRC, its binding partners, and the molecular mechanisms by which they function will help clarify the inner ear structures involved in the production of cochlear distortions.

In this study, we also assigned a protective function to the HTCs. Outer hair cells are the most vulnerable components of the hearing system. The stereocilia bundles are the primary site of injury following loud noise exposure. Such injuries typically reduce bundle stiffness (35). Our results indicate that the HTCs provide mechanical support to stereocilia, preventing injury. They do so by tying stereociliary bundles to one another within and between rows, connecting all of the stereocilia of each hair cell together as a unit. This seems to increase bundle sturdiness and prevent the splaying of the stereocilia that can occur with repeated acoustic insults. Similarly, the reduced bundle sturdiness that occurs when HTCs are defective likely increases susceptibility to age-related hearing loss. Consistent with this hypothesis, computational models of stereociliary bundle mechanics suggest that the lateral links connecting upper stereocilia to one another are likely to contribute most to bundle stiffness, improving their resistance to intense sound-induced damage (36). Moreover, another recent report implicated the HTCs in the maturation and maintenance of OHC bundle stiffness (37). Collectively, these findings suggest that HTCs are important in the pathogenesis of both genetic and environmental hearing impairments. Until recently, STRC was the only molecular component that had been associated with the HTCs. However, Avan et al. (38) reported that otogelin and otogelin-like are also components of the HTCs. STRC, otogelin, and otogelin-like are all secretory proteins. TUB also undergoes unconventional secretion in neuronal cell lines (39). Because both otogelin and otogelin-like disappear from OHC stereocilia in the absence of STRC (38), their expression in HTCs and TM-ACs should be likewise dependent on TUB. Further identification of the molecular composition of HTCs will greatly facilitate our understanding of the roles that HTCs play in bundle stiffness and may also reveal potential therapeutic targets for noise-induced hearing loss.

The auditory phenotypes of *Strc* KO mice and *tubby* mice appear to be identical, suggesting that these two molecules are tightly linked in stereocilia and in their role in normal hearing. It remains unclear how TUB protein determines the stereociliary localization of STRC in this study. The role that TUB plays in regulating the localization of various proteins in the primary cilia, which are microtubule-based sensory organelles extending from the cell surface, is more well studied. For example, TUB protein is required for the ciliary trafficking of somatostatin receptor 3 and melanin concentrating hormone receptor 1 in mice (40) and Inactive and NompC in *Drosophila* (25). In addition, the tubby family protein Tulp3 is required for the ciliary trafficking of at least 16 class A GPCRs (24) as well as the small GTPase ARL13B (41). The interaction of tubby family proteins with IFT-A components is critical for their regulation of the trafficking of membrane proteins in primary cilia (42). Unlike in primary cilia, there are no reports on the role that tubby family proteins play in stereocilia, which are actin-based structures. Thus, this report extends the role of TUB to actin-based organelles and suggests that TUB can regulate protein localization via another mechanism that is distinct from that occurring in primary cilia.

Another hint that TUB is a versatile molecule in both stereocilia and primary cilia comes from the close relationship between tubby family proteins and ciliary membrane phospholipids. In *Caenorhabditis elegans*, the tubby homolog TUB-1 regulates the membranous phosphoinositide composition of primary cilia (43). In mice and flies, tubby family proteins have a characteristic phosphoinositide-binding motif, and their function in the regulation of protein localization in primary cilia requires the interaction of this motif with membrane phosphoinositide (42, 44). Stereocilia may share a similar regulatory mechanism because we found that TUB protein is displaced from stereocilia when stereociliary membranes are depleted of PIP_2. It remains unclear, however, how TUB is delivered to stereocilia, how it interacts with

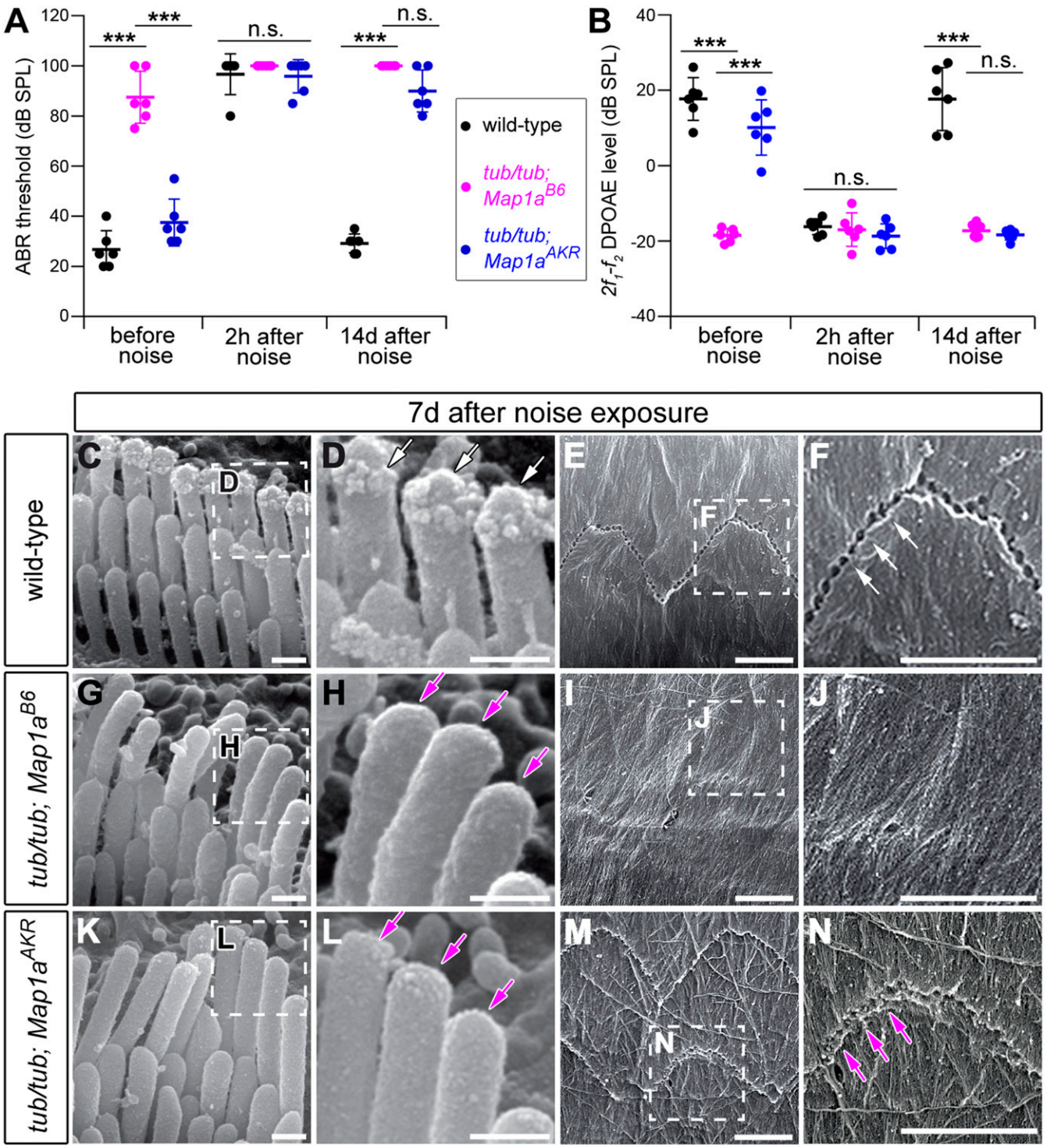

Fig. 4. HTCs are crucial for the resistance of hearing against acoustic trauma. (*A*) ABR thresholds for a click stimulus before, 2 h after, and 14 d after noise exposure (105 dB SPL for 2 h) in 5-wk-old wild-type mice ($n = 6$), *tub/tub; Map1a*^{B6} mice ($n = 6$), and *tub/tub; Map1a*^{AKR} mice ($n = 6$). (*B*) DPOAE amplitudes at $2f_1$-f_2 frequency ($f_1 = 10.871$ kHz, 65 dB SPL; $f_2 = 13.065$ kHz, 55 dB SPL) before, 2 h after, and 14 d after noise exposure (105 dB SPL for 2 h) in wild-type ($n = 6$), *tub/tub; Map1a*^{B6} ($n = 6$), and *tub/tub; Map1a*^{AKR} mice ($n = 6$). ABR and DPOAE data are plotted as interleaved scatter graphs in which individual dots represent individual data values and horizontal lines are means ± SD. Statistical comparisons were made with two-way ANOVA using Bonferroni corrections for multiple comparisons (***$P < 0.001$; n.s.: nonsignificant [$P > 0.05$]). (*C*, *D*, *G*, *H*, *K*, and *L*) SEM images of OHC stereocilia 7 d after noise exposure. The presence and absence of TM-ACs are indicated by white and magenta arrows, respectively. (*E*, *F*, *I*, *J*, *M*, and *N*) SEM images of the imprints on the undersurface of the TM 7 d after noise exposure. The distinct and less obvious imprints are indicated by white and magenta arrows, respectively. (Scale bars: 0.2 μm, *C*, *D*, *G*, *H*, *K*, and *L*; 2 μm, *E*, *F*, *I*, *J*, *M*, and *N*.)

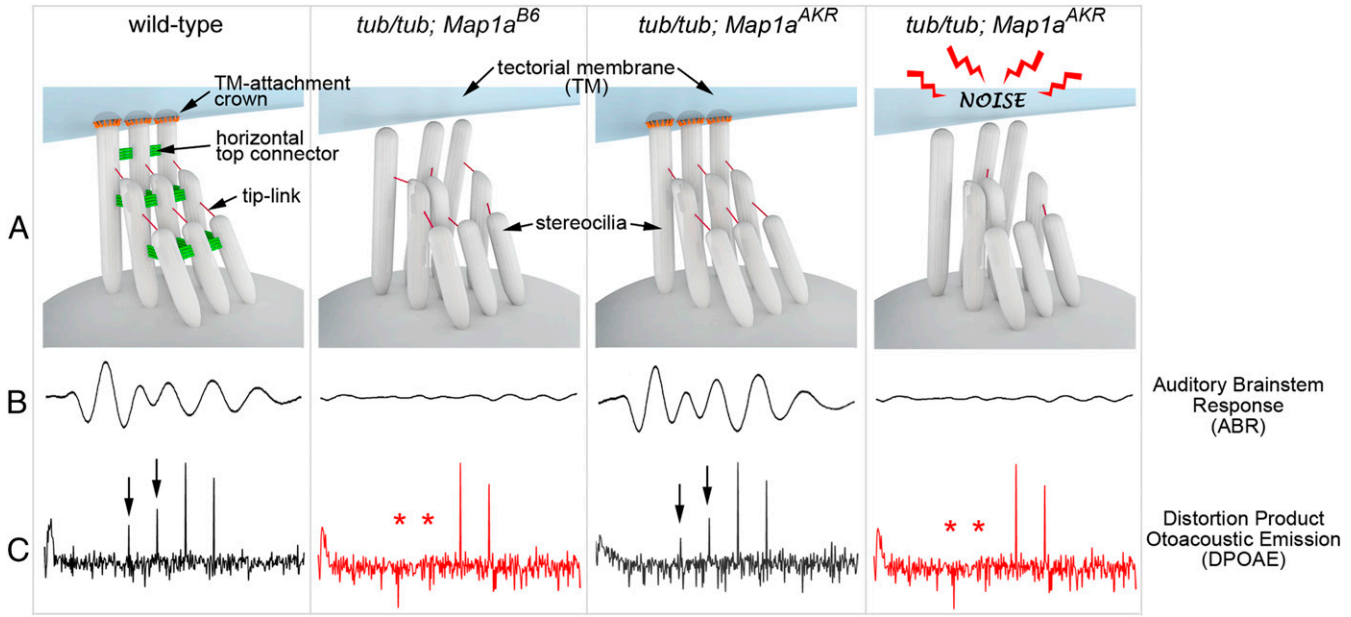

Fig. 5. Summary diagram illustrating the genotype-phenotype configuration in the OHCs of wild-type, *tub/tub; Map1a*^{B6}, and *tub/tub; Map1a*^{AKR} mice with or without noise exposure. (*A*) Schematic diagrams of the stereociliary structure in each genotype. (*B*) Representative ABR waveforms illustrating their presence or absence in each genotype. (*C*) Representative DPOAE peaks illustrating their presence (black arrows) or absence (red asterisks) in each genotype.

STRC, and how it affects STRC localization so that it can contribute to the establishment and maintenance of HTCs and TM-ACs. We hope to address these questions in future studies to expand our understanding of how tubby family proteins precisely regulate protein localization in tiny hair-like structures such as primary cilia and stereocilia across different tissues.

Materials and Methods

Tubby and AKR/N mice were purchased from The Jackson Laboratory (catalog # 000562) and Japan SLC (catalog # SLC-M-0248), respectively. Immunofluorescence staining, scanning electron microscopy, and in situ hybridization were performed as previously described (11, 45). ABRs and DPOAEs were measured in a sound-proof chamber using Tucker-Davis Technologies (TDT) RZ6 digital signal processing hardware and the BioSigRZ software package. Detailed materials and methods appear in *SI Appendix, Materials and Methods*.

Data Availability. All relevant data are included in this paper and *SI Appendix*.

ACKNOWLEDGMENTS. We thank Dr. Doris K. Wu and Dr. Jung-Bum Shin for critical reading of the manuscript, Ms. Hyeon-Joo Kim for assistance with illustrations, and Yonsei-Carl Zeiss Advanced Imaging Center at Yonsei University College of Medicine for technical assistance. This research was supported by the Brain Research Program through the National Research Foundation of Korea funded by Ministry of Science, Information and Communications Technology (ICT), and Future Planning (MSIT) Grants 2016M3C7A1913844 and 2015M3C7A1028396 (to C.H.K.); National Research Foundation of Korea Grant funded by the Korean Government (MSIT) Grants NRF-2018R1A5A2025079 and NRF-2019R1A2C3002354 (to C.H.K.) and Grants NRF-2014M3A9D5A01073865, NRF-2016R1A5A2008630, and NRF-2017R1A2B3009133 (to J.B.); Daegu Gyeongbuk Institute of Science and Technology R&D Program of the Ministry of Science, ICT, and Future Planning Grant 18-BD-06 (to C.H.K. and D.W.M.).

1. J. Ashmore *et al*., The remarkable cochlear amplifier. *Hear. Res.* **266**, 1–17 (2010).
2. P. G. Gillespie, U. Müller, Mechanotransduction by hair cells: Models, molecules, and mechanisms. *Cell* **139**, 33–44 (2009).
3. A. J. Hudspeth, Integrating the active process of hair cells with cochlear function. *Nat. Rev. Neurosci.* **15**, 600–614 (2014).
4. N. A. Lesica, Why do hearing aids fail to restore normal auditory perception? *Trends Neurosci.* **41**, 174–185 (2018).
5. G. K. Martin, B. B. Stagner, B. L. Lonsbury-Martin, Assessment of cochlear function in mice: Distortion-product otoacoustic emissions. *Curr. Protoc. Neurosci.* **Chapter 8**, Unit8 21C (2006).
6. R. J. Goodyear, W. Marcotti, C. J. Kros, G. P. Richardson, Development and properties of stereociliary link types in hair cells of the mouse cochlea. *J. Comp. Neurol.* **485**, 75–85 (2005).
7. P. Avan, B. Büki, C. Petit, Auditory distortions: Origins and functions. *Physiol. Rev.* **93**, 1563–1619 (2013).
8. P. K. Legan *et al*., A targeted deletion in alpha-tectorin reveals that the tectorial membrane is required for the gain and timing of cochlear feedback. *Neuron* **28**, 273–285 (2000).
9. A. N. Lukashkin, V. A. Lukashkina, P. K. Legan, G. P. Richardson, I. J. Russell, Role of the tectorial membrane revealed by otoacoustic emissions recorded from wild-type and transgenic Tecta(deltaENT/deltaENT) mice. *J. Neurophysiol.* **91**, 163–171 (2004).
10. E. Verpy *et al*., Stereocilin connects outer hair cell stereocilia to one another and to the tectorial membrane. *J. Comp. Neurol.* **519**, 194–210 (2011).
11. E. Verpy *et al*., Stereocilin-deficient mice reveal the origin of cochlear waveform distortions. *Nature* **456**, 255–258 (2008).
12. D. L. Coleman, E. M. Eicher, Fat (fat) and tubby (tub): Two autosomal recessive mutations causing obesity syndromes in the mouse. *J. Hered.* **81**, 424–427 (1990).
13. J. R. Heckenlively *et al*., Mouse model for Usher syndrome: Linkage mapping suggests homology to Usher type I reported at human chromosome 11p15. *Proc. Natl. Acad. Sci. U.S.A.* **92**, 11100–11104 (1995).
14. P. W. Kleyn *et al*., Identification and characterization of the mouse obesity gene tubby: A member of a novel gene family. *Cell* **85**, 281–290 (1996).
15. K. Noben-Trauth, J. K. Naggert, M. A. North, P. M. Nishina, A candidate gene for the mouse mutation tubby. *Nature* **380**, 534–538 (1996).
16. S. Santagata *et al*., G-protein signaling through tubby proteins. *Science* **292**, 2041–2050 (2001).
17. K. Carroll, C. Gomez, L. Shapiro, Tubby proteins: The plot thickens. *Nat. Rev. Mol. Cell Biol.* **5**, 55–63 (2004).
18. S. Mukhopadhyay, P. K. Jackson, The tubby family proteins. *Genome Biol.* **12**, 225 (2011).
19. T. J. Boggon, W. S. Shan, S. Santagata, S. C. Myers, L. Shapiro, Implication of tubby proteins as transcription factors by structure-based functional analysis. *Science* **286**, 2119–2125 (1999).
20. A. Ikeda *et al*., Microtubule-associated protein 1A is a modifier of tubby hearing (moth1). *Nat. Genet.* **30**, 401–405 (2002).
21. N. B. Caberoy, Y. Zhou, W. Li, Tubby and tubby-like protein 1 are new MerTK ligands for phagocytosis. *EMBO J.* **29**, 3898–3910 (2010).
22. R. Kapeller *et al*., Tyrosine phosphorylation of tub and its association with Src homology 2 domain-containing proteins implicate tub in intracellular signaling by insulin. *J. Biol. Chem.* **274**, 24980–24986 (1999).
23. A. Mukhopadhyay, X. Pan, D. G. Lambright, H. A. Tissenbaum, An endocytic pathway as a target of tubby for regulation of fat storage. *EMBO Rep.* **8**, 931–938 (2007).
24. H. B. Badgandi, S. H. Hwang, I. S. Shimada, E. Loriot, S. Mukhopadhyay, Tubby family proteins are adapters for ciliary trafficking of integral membrane proteins. *J. Cell Biol.* **216**, 743–760 (2017).

25. J. Park *et al*., dTULP, the Drosophila melanogaster homolog of tubby, regulates transient receptor potential channel localization in cilia. *PLoS Genet.* **9**, e1003814 (2013).
26. K. K. Ohlemiller *et al*., Progression of cochlear and retinal degeneration in the tubby (rd5) mouse. *Audiol. Neurotol.* **2**, 175–185 (1997).
27. L. Kong *et al*., Molecular mechanisms underlying cochlear degeneration in the tubby mouse and the therapeutic effect of sulforaphane. *Neurochem. Int.* **54**, 172–179 (2009).
28. A. Ikeda *et al*., Genetic modification of hearing in tubby mice: Evidence for the existence of a major gene (moth1) which protects tubby mice from hearing loss. *Hum. Mol. Genet.* **8**, 1761–1767 (1999).
29. E. Verpy *et al*., Mutations in a new gene encoding a protein of the hair bundle cause non-syndromic deafness at the DFNB16 locus. *Nat. Genet.* **29**, 345–349 (2001).
30. J. Zheng *et al*., Prestin is the motor protein of cochlear outer hair cells. *Nature* **405**, 149–155 (2000).
31. K. D. Karavitaki, D. P. Corey, Sliding adhesion confers coherent motion to hair cell stereocilia and parallel gating to transduction channels. *J. Neurosci.* **30**, 9051–9063 (2010).
32. A. S. Kozlov, J. Baumgart, T. Risler, C. P. Versteegh, A. J. Hudspeth, Forces between clustered stereocilia minimize friction in the ear on a subnanometre scale. *Nature* **474**, 376–379 (2011).
33. J. A. Clark, J. O. Pickles, The effects of moderate and low levels of acoustic overstimulation on stereocilia and their tip links in the guinea pig. *Hear. Res.* **99**, 119–128 (1996).
34. V. Tsuprun, P. A. Schachern, S. Cureoglu, M. Paparella, Structure of the stereocilia side links and morphology of auditory hair bundle in relation to noise exposure in the chinchilla. *J. Neurocytol.* **32**, 1117–1128 (2003).
35. R. K. Duncan, J. C. Saunders, Stereocilium injury mediates hair bundle stiffness loss and recovery following intense water-jet stimulation. *J. Comp. Physiol. A Neuroethol. Sens. Neural Behav. Physiol.* **186**, 1095–1106 (2000).
36. J. Cotton, W. Grant, Computational models of hair cell bundle mechanics: II. Simplified bundle models. *Hear. Res.* **197**, 105–111 (2004).
37. A. X. Cartagena-Rivera, S. Le Gal, K. Richards, E. Verpy, R. S. Chadwick, Cochlear outer hair cell horizontal top connectors mediate mature stereocilia bundle mechanics. *Sci. Adv.* **5**, eaat9934 (2019).
38. P. Avan *et al*., Otogelin, otogelin-like, and stereocilin form links connecting outer hair cell stereocilia to each other and the tectorial membrane. *Proc. Natl. Acad. Sci. U.S.A.* **116**, 25948–25957 (2019).
39. N. B. Caberoy, W. Li, Unconventional secretion of tubby and tubby-like protein 1. *FEBS Lett.* **583**, 3057–3062 (2009).
40. X. Sun *et al*., Tubby is required for trafficking G protein-coupled receptors to neuronal cilia. *Cilia* **1**, 21 (2012).
41. S. H. Hwang *et al*., Tulp3 regulates renal cystogenesis by trafficking of cystoproteins to Cilia. *Curr. Biol.: CB* **29**, 790–802.e5 (2019).
42. S. Mukhopadhyay *et al*., TULP3 bridges the IFT-A complex and membrane phosphoinositides to promote trafficking of G protein-coupled receptors into primary cilia. *Genes Dev.* **24**, 2180–2193 (2010).
43. D. DiTirro, A. Philbrook, K. Rubino, P. Sengupta, The *Caenorhabditis elegans* Tubby homolog dynamically modulates olfactory cilia membrane morphogenesis and phospholipid composition. *eLife* **8**, e48789 (2019).
44. J. Park *et al*., Ciliary phosphoinositide regulates ciliary protein trafficking in Drosophila. *Cell Rep.* **13**, 2808–2816 (2015).
45. E. J. Son *et al*., Conserved role of Sonic Hedgehog in tonotopic organization of the avian basilar papilla and mammalian cochlea. *Proc. Natl. Acad. Sci. U.S.A.* **112**, 3746–3751 (2015).